DOI 10.5012/bkcs.2011.32.8.2787

Donor-Acceptor-Donor Type Red Fluorescent Emitters Containing Adamandane-substituted Julolidines for OLEDs

Kum Hee Lee, Young Kwan Kim,†,* and Seung Soo Yoon*

*Department of Chemistry, Sungkyunkwan University, Suwon 440-746, Korea. *E-mail: ssyoon@skku.edu*
*†Department of Information Display, Hongik University, Seoul 121-791, Korea. *E-mail: kimyk@hongik.ac.kr*
Received May 19, 2011, Accepted June 16, 2011

Key Words : Red OLEDs, Adamandane-substituted, Julolidine, Donor-acceptor-donor type materials

Organic light-emitting diodes (OLEDs) have attracted much attention given their advantages to self-emission of light, wide angle, and applications in flat-panel displays. Red, green, and blue OLEDs with high efficiencies and low device driving voltages are necessary for full color displays.[1] In red fluorescent OLEDs, donor-acceptor type materials such as 4-(dicyanomethylene)-2-methyl-6-[*p*-(dimethylamino)styryl]-4*H*-pyran (DCM) derivatives have been widely used as red fluorescent emitters.[2-8]

In this paper, a series of donor-acceptor-donor red fluorescent emitters (**1-4**) were synthesized and their electroluminescent properties were investigated. In compounds **1-4**, the bulky adamantane groups were incorporated in donor moieties in order to prevent molecular aggregation between emitters, thus reducing concentration quenching. Compared to the simple donor-acceptor type materials such as DCM derivatives, these donor-acceptor-donor type materials (**1-4**) are expected to show improved color chromaticity due to the extended π-conjugation length. In addition, to study the structural effects of emitters on EL performance, various acceptor moieties containing –CN groups were introduced into red fluorescent materials **1-4**.

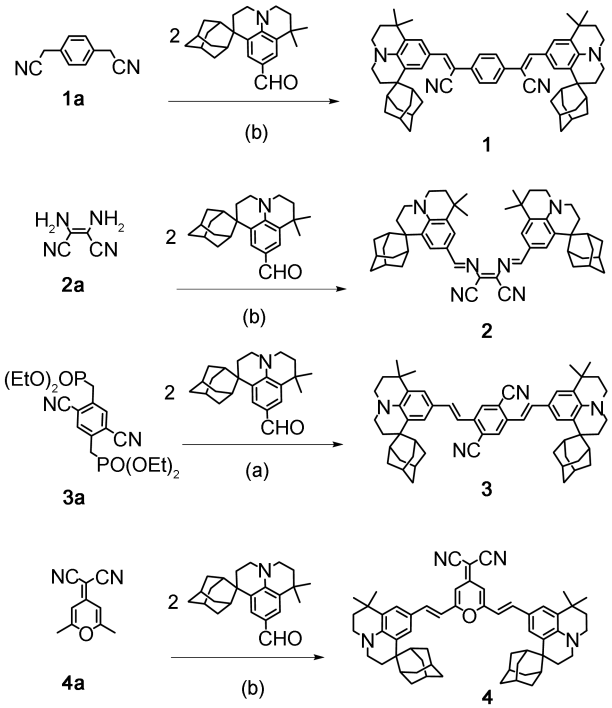

Scheme 1. Synthetic routes of red materials (**1-4**). *Condition*: (a) Piperidine, EtOH, reflux, 24 h, (b) 1.0 M KO*t*-Bu, THF, 0 °C → rt, 1 h.

Usually, doping is used to obtain red emissions, in which the emitting layer is compose of a host and red dopant in order to prevent concentration quenching in the emitting layer.[9-12] Recently, a co-host system was reported to overcome the incomplete energy transfer between host and dopant.[13-16] In this study, rubrene is employed as an assistant host in order to enhance energy transfer from host to dopants and thus improve the EL efficiencies.

Scheme 1 shows the synthetic route of the designed donor-acceptor-donor type red fluorescent emitters. 5-(3-Adamantyl-7,7-dimethyljulolidyl)carbaldehyde was prepared through Vilsmeier reaction. Compounds **1**, **2**, and **4** were prepared by the Knoevenagel condensation of aldehyde with the corresponding active methylene compounds (**1a**, **2a**, and **4a**). The reaction of aldehyde with phosphonate intermediates (**3a**) gave **3** by the Horner-Emmons reaction.

The UV-vis absorption and PL spectra of red materials **1-4** are shown in Figure 1. The photophysical properties of **1-4** are summarized in Table 1. Compound **2**, having phenylenediacetonitrile moiety as a acceptor, shows the longest maximum absorption and emission peak of 587 and 648 nm, respectively, while compound **1**, having diaminomaleonitrile

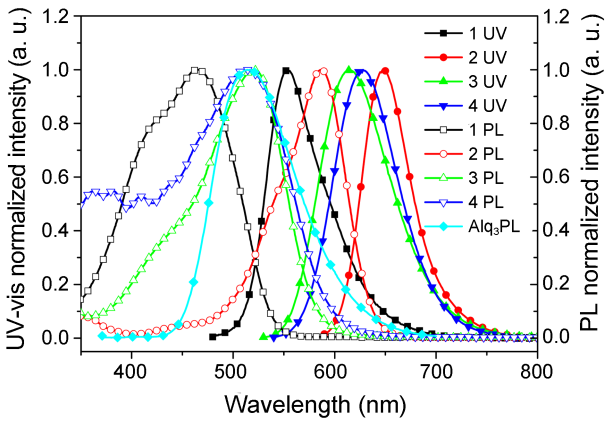

Figure 1. UV-vis absorption and PL emission spectra of red emitters (**1-4**).

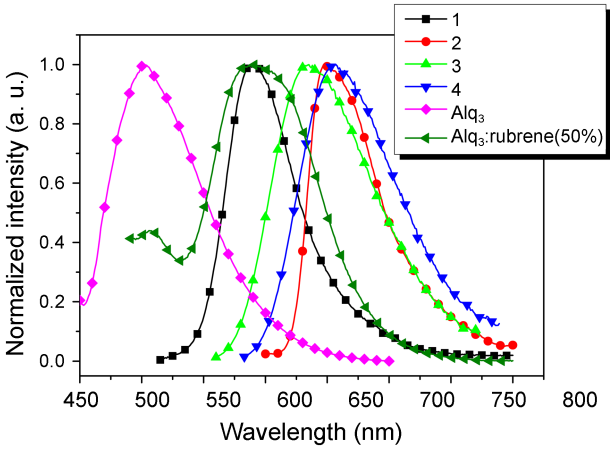

Figure 2. Solid PL spectra of the Alq_3: rubrene (50%) doped with dopant **1-4** at doping concentration of 2%.

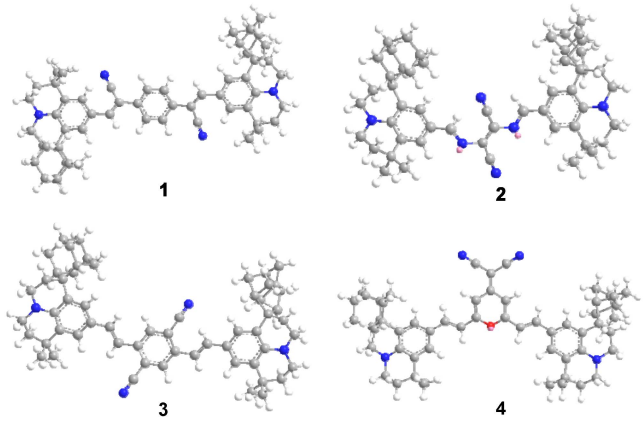

Figure 3. Energy-minimized structure of compounds (**1-4**) by standard MM2 calculation.

moiety as a acceptor, shows the shortest ones of 464 and 553 nm, respectively. Moreover, compared to **1**, the maximum emission peak of **3** was red shifted (*ca*. 62 nm) owing to the cyano group of **3** lies in conjugation with the distant julolidine moiety whereas those of **1** will conjugate with proximate julolidine moiety. The absorption of each compound shows a good spectral overlap with the emission of the host (Alq_3). This indicates that Alq_3 serves as a suitable host in the OLEDs using the compounds **1-4** as red dopant materials. These red emitters **1-4** show FWHM of 65, 55, 82, and 74 nm, respectively. The PL quantum yields of **1-4** were measured in 1,2-dichloroethane, using DCJTB as the standard, and were found to be 0.01-0.46, respectively. Interestingly, the quantum yield of **3** (0.37) and **4** (0.46) were higher than those of **1** and **2**. Therefore, **3** and **4** could be quite good as a red dopant for OLEDs.

Figure 2 shows the solid PL spectra of the Alq_3:rubrene (50%) host doped with dopant **1-4** film at doping concentration of 2%. The maximum emission peaks of **1-4** were 588, 647, 635, and 657 nm, respectively. The Alq_3 and Alq_3: rubrene (50%) film showed PL emission at 502 and 588 nm, the Alq_3: rubrene (50%) emission disappeared in the Alq_3: rubrene (50%) film doped with dopants **2-4**. This confirms the efficient energy transfer from the Alq_3: rubrene (50%) host to the dopant materials. Interestingly, compared to the solid PL spectra of Alq_3: rubrene (50%), Alq_3: rubrene (50%) doped with dopant **1** film showed same wavelength. This imply that the energy transfer from rubrene to dopant **1** is ineffective due to the smaller band-gap of rubrene (2.20 eV) than that of dopant **1** (2.38 eV). However, the energy transfer from Alq_3 to dopant **1** is possible. Presumably, the PL spectrum of Alq_3: rubrene (50%) film doped with dopant **1** is composed of emissions from dopant **1** as well as rubrene. Intriguingly, the PL spectrum of Alq_3: rubrene (50%) film doped with dopant **4** showed the longer emission wavelength than that doped with dopant **2** in spite that the solution PL spectrum of **4** showed the shorter emission wavelength than that of **2**. This suggests that the emission of of Alq_3: rubrene (50%) film doped with dopant **4** originated from the excimer of **4** through the effective molecular aggregation of **4**.

Molecular simulations studies of compounds **1-4** using molecular mechanics (MM2) energy minimization were carried out to test the tendency of molecular aggregation and thus the excimer formation of **1-4** at the molecular level. Figure 3 shows the energy minimized structures of compounds **1-4**. The calculated angles between the adamantane-substituted phenyl rings and the central phenyl rings at energy-minimized structures of compounds **1**, **3** and **4** increased in the order of **4** (3°) < **1** (25°) < **3** (37°). In addition, the imine center group of compound **2** would provide large steric hindrance for molecular aggregation, in which the calculated angle between the adamantane-substituted phenyl rings was 53°. This suggests that intermolecular aggregation was suppressed in the order **4** < **1** < **3** < **2** and the excimer formation was effective in the reverse order. The HOMO energy levels for red materials **1-4** were measured by a low-energy photoelectron spectrometer (Riken-Keiki AC-2). Their HOMO/LUMO energy levels were −5.49/−3.11, −5.31/−3.31, −5.66/−3.48, and −5.79/−3.66, respectively. These results indicate that the energy levels were very sensitive to the structural features of the acceptor moieties. For example, compared to **1** with the cyano groups in the vinyl bridge, the energy levels of **3** with those in the phenylene core had lower values. Also, in the case of **4** with pyran core unit, its energy levels exhibit the lowest value. The optical energy band gaps (E_g) of **1-4**

Table 1. Physical properties of red emitters (**1-4**)

Compound	UV_{max}[a] (nm)	PL_{max}[a] (nm)	FWHM	HOMO/LUMO[b] (eV)	E_g	Q.Y[c]	mp (°C)
1	464	553	65	-5.49/-3.11	2.38	0.01	205
2	587	648	55	-5.31/-3.31	2.00	0.23	308
3	520	615	82	-5.66/-3.48	2.18	0.37	283
4	513	628	74	-5.79/-3.66	2.13	0.46	> 320

[a,b]Maximum absorption or emission wavelength in 1,2-dichloroethane (1×10^{-5} M). [b]Obtained from AC-2 and UV-vis absorption measurements. [c]Using DCJTB as a standard; λ_{ex} = 550 nm (Φ = 0.78 in 1,2-dichloroethene).

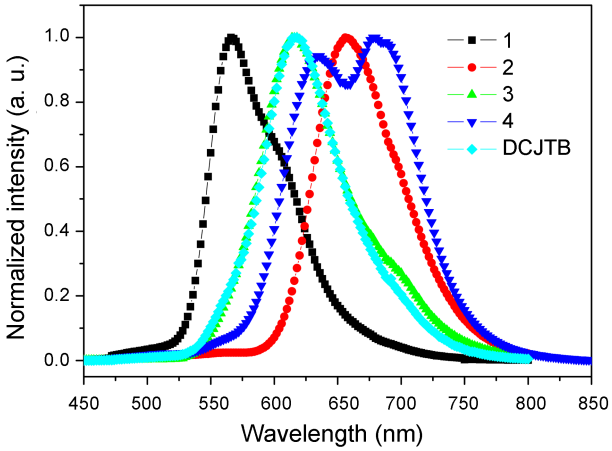

Figure 4. EL spectra at 8.0 V of the devices **1-4**.

were 2.38, 2.00, 2.18, and 2.13 eV, respectively, as determined from the absorption and photoluminescence spectra.

To explore the electroluminescent properties of the red fluorescent materials, devices were fabricated with structure of ITO/NPB (40 nm)/Alq_3: rubrene (50%): **1-4** (2%) (20 nm)/Alq_3 (40 nm)/Liq (1 nm)/Al (100 nm). For comparison, we also fabricated the corresponding red-emitting device using DCJTB as a dopant at the same doping concentration. The electroluminescent properties of the devices of **1-4** and DCJTB are summarized in Table 2. While device **1** showed orange emissions with peaks at 566 nm, devices **2** and **3** showed red emissions with peaks at 656 and 618 nm, as shown in Figure 4. Device **2** had a very red-shifted wavelength at 656 nm in the EL spectra. The device **4** has emission peak at 635 nm in EL spectra; however, the shoulder peak due to excimer formation takes place around 678 nm. At a driving voltage of 8.0 V, the CIE coordinates of **1-4** based devices are (0.52, 0.48), (0.68, 0.32), (0.63, 0.33), and (0.66, 0.33), respectively. Interestingly, devices **2** and **4** showed the CIE coordinates which were close to the NTSC red standard of (0.67, 0.33).

The luminous efficiencies (LE) and power efficiencies (PE) of red devices **1-4** and DCJTB are shown in Figure 5 and

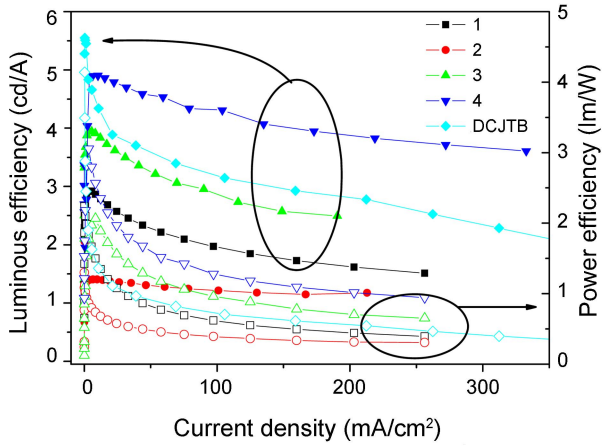

Figure 5. The luminous and power efficiencies versus current density relationship of the devices **1-4** (closed: LE, opened: PE).

Table 2. EL performance characteristic of red OLEDs

Device	L[a] (cd/m²)	V_{on}[b] (V)	LE[c] (cd/A)	PE[c] (lm/W)	EL[e] (nm)	FWHM	CIE[d] (x,y)
1	3875	2.7	2.64	1.16	566	71	(0.52, 0.48)
2	2497	3.1	1.37	0.57	656	79	(0.68, 0.32)
3	4749	2.9	3.67	1.50	618	76	(0.63, 0.33)
4	12010	2.6	4.81	2.20	635, 678	115	(0.66, 0.33)
DCJTB	7600	3.0	3.88	1.11	616	73	(0.61, 0.39)

[a]Value of luminance at 12.0 V. [b]Turn-on voltage at 1.0 cd/m². [c]Value measured at 20 mA/cm². [d]Value measured at 8.0 V.

key device performance parameters are summarized in Table 2. Notably, the luminance of the device **4** is 2-5 times higher than the others. Among those, device **4** exhibits the most efficient emission with the luminous efficiency of 4.81 cd/A at 20 mA/cm² with a power efficiency of 2.20 lm/W. This result may be attributed higher fluorescence quantum yield of **4** than **1**, **2**, and **3**. Interestingly, compared to device **2**, device **1** showed the improved EL efficiencies in spite that the fluorescence quantum yield of dopant **1** is much smaller than that of dopant **2**. Presumably, the emission of device **1** originated from dopant **1** as well as rubrene because the energy transfer from rubrene to dopant **1** is ineffective due to the smaller band-gap of rubrene (2.20 eV) than that of dopant **1** (2.38 eV). The efficient emission from rubrene would contribute the improved EL efficiencies of device **1** as compared to device **2**. Notably, compared with device using **DCJTB**, device **4** showed the improved EL performances. For example, the luminous and power efficiencies of device **4** increased by 24 and 98% at 20 mA/cm², respectively, as compared to device using DCJTB. Also, device **4** exhibited the better CIE coordinates (0.66, 0.33) than DCJTB-based device (0.61, 0.39). Thus, this study demonstrates that the donor-acceptor-donor type materials are excellent candidates for use as red fluorescent emitters in OLEDs.

In conclusion, a series of donor-acceptor-donor red fluorescent emitters (**1-4**) have been synthesized and their electroluminescent properties were investigated. All devices using these materials as dopants in Alq_3/rubrene co-host emitting layer showed the efficient red electroluminescence. In particular, a device containing emitter **4** as a dopant demonstrated a luminance, luminous, and power efficiency of 12010 cd/m², 4.81 cd/A and 2.20 lm/W at 20 mA/cm², respectively, with CIE *x*, *y* coordinates of (0.66, 0.33) at 8.0 V. The deep red device **2** showed CIE *x*, *y* coordinates of (0.68, 0.32) at 8.0 V, a luminous efficiency of 1.37 cd/A, and power efficiency of 0.57 lm/W at 20 mA/cm².

Experimental Section

Materials and Measurement. 1,4-Phenylenediacetonitrile (**1a**), diaminomaleonitrile (**2a**), and 4-(dicyanomethylene)-2,6-dimethyl-4*H*-pyran (**4a**) were used as received from Aldrich or TCI Co. Tetraethyl-(2,5-dicyano-α,α'-*p*-xylylenediphosphonate) (**3a**) and 5-(3-adamantyl-7,7-dimethyljulolidyl)carbaldehyde were synthesized as reported previ-

ously.[17]

General Procedure: Type I. Into a round-bottom flask was added 5-(3-adamantyl-7,7-dimethyljulolidyl)carbaldehyde (2.1 mmol) and **1a** or **2a** or **4a** (1.0 mmol), respectively, which was then fitted with a deanstark trap (packed with molecular sieves) and reflux condenser. Anhydrous ethanol and piperidine (10.0 mmol) were then added and heated to 110 °C for 24 h and cooled in a refrigerator. The mixture was filtered and extracted with ethyl acetate and washed with water. After filtration and solvent evaporation, the mixture was purified by recrystallization from dichloromethane and hexane.

Synthesis of 1. Yield: 45.6%. ^{1}H-NMR (300 MHz, $CDCl_3$) δ 7.90 (d, J = 1.8 Hz, 2H), 7.75 (d, J = 1.8 Hz, 2H), 7.64 (s, 4H), 7.41 (s, 2H), 3.26 (q, J = 6.6 Hz, 8H), 2.27-2.15 (m, 12H), 2.05-2.03 (m, 4H), 1.95-1.90 (m, 4H), 1.80-1.70 (m, 16H), 1.33 (s, 12H). ^{13}C-NMR (75 MHz, $CDCl_3$) δ 143.9, 143.7, 135.4, 130.7, 130.6, 126.8, 125.7, 120.1, 119.9, 101.4, 46.3, 46.1, 41.4, 39.5, 36.3, 35.0, 33.9, 32.3, 32.2, 31.3, 30.3, 28.3, 28.0. FT-IR: ν 2910, 2349, 1605, 1521, 1322, 1225, 989, 834 cm^{-1}. MS (FAB, *m/z*): 819 [M$^+$]; HRMS: [EI$^+$] calcd for $C_{58}H_{66}N_4$: 818.5288, [M$^+$]. Found: 818.5285.

Synthesis of 2. Yield: 54.1%. ^{1}H-NMR (300 MHz, $CDCl_3$) δ 8.50 (s, 2H), 7.94 (s, 2H), 7.62 (s, 2H), 3.26 (q, J = 6.6 Hz, 8H), 2.26-2.18 (m, 8H), 2.11-2.03 (m, 10H), 1.95-1.92 (m, 14H), 1.31 (s, 10H). FT-IR: ν 2970, 1739, 1366, 1217 cm^{-1}. MS (FAB, *m/z*): 771 [M$^+$]; HRMS: [EI$^+$] calcd for $C_{52}H_{62}N_6$: 770.5036, [M$^+$]. Found: 770.5041.

Synthesis of 4. Yield: 30.7%. ^{1}H-NMR (300 MHz, $CDCl_3$) δ 7.94 (s, 2H), 7.50 (s, 2H), 7.27 (s, 2H), 7.21 (d, J = 15.9 Hz, 2H), 7.05 (d, J = 15.9 Hz, 2H), 3.22 (d, J = 5.1 Hz, 7H), 2.28-2.17 (m, 12H), 2.01-1.90 (m, 9H), 1.76-1.70 (m, 16H), 1.31 (s, 12H). ^{13}C-NMR (75 MHz, $CDCl_3$) δ 142.4, 138.7, 135.9, 131.0, 129.0, 124.4, 122.7, 121.8, 117.6, 115.6, 113.8, 46.4, 46.0, 41.5, 39.5, 36.6, 35.0, 33.9, 32.3, 32.2, 31.4, 30.4, 28.4, 28.1. FT-IR: ν 2913, 2210, 1660, 1552, 1181, 971, 866 cm^{-1}. MS (FAB, *m/z*): 834 [M$^+$]; HRMS: [EI$^+$] calcd for $C_{58}H_{66}N_4O$: 834.5237, [M$^+$]. Found 834.5233.

General Procedure: Type II. To a mixture of 5-(3-adamantyl-7,7-dimethyljulolidyl)carbaldehyde (2.2 mmol) and **3a** (1.0 mmol) in anhydrous THF at 0 °C was added dropwise 1.0 M KO*t*-Bu (2.4 mmol) in THF under an Ar atmosphere. The reaction mixture was stirred for 10 min at 0 °C followed by 1 h at room temperature. After the reaction had finished, the reaction mixture was extracted with ethyl acetate and washed with water. The organic layer was dried with anhydrous $MgSO_4$ and filtered. The mixture was evaporated and the residue purified by recrystallization from dichloromethane and hexane.

Synthesis of 3. Yield: 38.5%. ^{1}H-NMR (300 MHz, $CDCl_3$) δ 7.94 (s, 2H), 7.50 (s, 2H), 7.27 (s, 2H), 7.21 (d, J = 15.9 Hz, 2H), 7.05 (d, J = 15.9 Hz, 2H), 3.22 (d, J = 5.1 Hz, 7H), 2.28-2.17 (m, 12H), 2.01-1.90 (m, 9H), 1.76-1.70 (m, 16H), 1.31 (s, 12H). ^{13}C-NMR (75 MHz, $CDCl_3$) δ 142.4, 138.7, 135.9, 131.0, 129.0, 124.4, 122.7, 121.8, 117.6, 115.6, 113.8, 46.4, 46.0, 41.5, 39.5, 36.6, 35.0, 33.9, 32.3, 32.2, 31.4, 30.4, 28.4, 28.1. FT-IR: ν 2910, 2360, 1593, 1321, 1224, 953 cm^{-1}. MS (FAB, *m/z*): 819 [M$^+$]; HRMS: [EI$^+$] calcd for $C_{58}H_{66}N_4$: 818.5288, [M$^+$]. Found: 818.5291.

OLED Fabrication and Measurement. The OLEDs using red-light-emitting molecules were fabricated by vacuum (10^{-6} torr) thermal evaporation onto pre-cleaned ITO-coated glass substrates. The structure was as follows: ITO/4,4'-bis(*N*-(1-naphthyl)-*N*-phenylamino)biphenyl (NPB) (40 nm)/ Red **1-4** (2%): rubrene (50%): tris(8-quionlinolato)-aluminium (Alq_3) (20 nm)/Alq_3 (40 nm)/Liq (1 nm)/Al (100 nm). All OLEDs properties such as the current density (*J*), luminance (*L*), luminance efficiency (LE) and Commission Internationale de I'Eclairage coordinates (CIE) coordinate characteristics were measured using a Keithly 2400 source measurement unit and Chroma meter MINOLTA CS-1000A. Electroluminance was measured using a Roper Scientific Pro 300i.

Acknowledgments. This research was supported by Basic Science Research Program through the National Research Foundation of Korea (NRF) funded by the Ministry of Education, Science and Technology (20110004655).

References and Notes

1. Tang, C. W.; VanSlyke, S. A.; Chen, C. H. *J. Appl. Phys*. **1989**, *65*, 3610.
2. Chen, C.-T. *Chem. Mater.* **2004**, *16*, 4389.
3. Lee, K. H.; Kim, S. M.; Kim, J. Y.; Kim, Y. K.; Yoon, S. S. *Bull. Korean. Chem. Soc*. **2010**, *31*, 2884.
4. Lee, K. H.; Park, M. H.; Kim, S. M.; Kim, Y. K.; Yoon, S. S. *Jpn. J. Appl. Phys.* **2010**, *49*, 08JG02.
5. Lee, K. H.; Kim, Y. K.; Yoon, S. S. *Bull. Korean. Chem. Soc*. **2011**, *32*, 1391.
6. Lee, K. H.; Park, M. H.; Kim, J. Y.; Kim, S. M.; Seo, B. M.; Seo, J. H.; Kim, Y. K.; Yoon, S. S. *J. Nanosci. Nanotechnol*. **2011**, *11*, 1484.
7. Zhao, P.; Tang, H.; Zhang, Q.; Pi, Y.; Xu, M.; Sun, R.; Zhu, W. *Dyes and Pigments* **2009**, *82*, 316.
8. Yao, Y.-S.; Zhou, Q.-X.; Wang, X.-S.; Wang, Y.; Zhang, B.-W. *Adv. Funct. Mater.* **2007**, *17*, 93.
9. Xie, Z. Y.; Hung, L. S.; Lee, S. T. *Appl. Phys. Lett*. **2001**, *79*, 1048.
10. List, E. J. W.; Tasch, S.; Hochfilzer, C.; Leising, G.; Schlichting, P.; Rohr, U.; Geerts, Y.; Scherf, U.; Müllen, K. *Opt. Mater.* **1998**, *9*, 183.
11. Jin, Y. D.; Yang, J. P.; Heremans, P. L.; Auweraer, M. V.; Rousseau, E.; Geise, H. J.; Borghs, G. *Chem. Phys. Lett*. **2000**, *320*, 387.
12. Feng, J.; Li, F.; Gao, W.; Cheng, G.; Xie, W.; Liu, S. *Appl. Phys. Lett*. **2002**, *81*, 2935.
13. Haq, K. U.; Liu, S. P.; Khan, M. A.; Jiang, X. Y.; Zhang, Z. L.; Zhu, W. Q. *Semicond. Sci. Technol.* **2008**, *23*, 035024.
14. Lee, T. W.; Park, O. O.; Cho, H. N.; Kim, Y. C. *Curr. Appl. Phys*. **2001**, *1*, 363.
15. D'Andrade, B. W.; Baldo, M. A.; Adachi, C.; Brooks, J. *Appl. Phys. Lett.* **2001**, *79*, 1045.
16. Hamada, Y.; Kanno, H.; Tsujioka, T.; Takahashi, H. *Appl. Phys. Lett*. **1999**, *75*, 1682.
17. Kim, B. O.; Kim, C. S.; Han H.; Kim S. M.; Kim, J. Y.; Cho, K, S.; Jung, S. Y.; Yun, S. S.; Kwon, H, J.; Cho, Y. J.; Kim, Y. K.; Kim, S. M. *WO 121274*, 2005.
18. Chen, C. H.; Tang, C. W.; Shi, J., Klubek, K. P. *Thin Solid Films* **2000**, *363*, 327.